Earthquakes and Structures, *Vol. 7, No. 4 (2014) 527-552*
DOI: http://dx.doi.org/10.12989/eas.2014.7.4.527

Experimental and theoretical studies of confined HSCFST columns under uni-axial compression

M.H. Lai[1] and J.C.M. Ho[*1]

[1]*Department of Civil Engineering, The University of Hong Kong, Hong Kong*
[2]*School of Civil Engineering, The University of Queensland, QLD 4072, Australia*

(Received may 5, 2014, Revised June 1, 2014, Accepted June 6, 2014)

Abstract. The development of modern concrete technology makes it much easier to produce high-strength concrete (HSC) or ultra-high-strength concrete (UHSC) with high workability. However, the application of this concrete is limited in practical construction of traditional reinforced concrete (RC) structures due to low-ductility performance. To further push up the limit of the design concrete strength, concrete-filled-steel-tube (CFST) columns have been recommended considering its superior strength and ductility performance. However, the beneficial composite action cannot be fully developed at early elastic stage as steel dilates more than concrete and thereby reducing the elastic strength and stiffness of the CFST columns. To resolve this problem, external confinement in the form of steel rings is proposed in this study to restrict the lateral dilation of concrete and steel. In this paper, a total of 29 high-strength CFST (HSCFST) columns of various dimensions cast with concrete strength of 75 to 120 MPa concrete and installed with external steel rings were tested under uni-axial compression. From the results, it can be concluded that the proposed ring installation can further improve both strength and ductility of HSCFST columns by restricting the column dilation. Lastly, an analytical model calculating the uni-axial strength of ring-confined HSCFST columns is proposed and verified based on the Von-Mises and Mohr-Coulomb failure criteria for steel tube and in-filled concrete, respectively.

Keywords: analytical model; concrete-filled-steel-tube; high-strength concrete; mohr-coulomb; von-mises

1. Introduction

The development of modern concrete technology makes it easier to produce high-strength concrete (HSC) or ultra-high-strength concrete (UHSC) with high workability. The possibility of using this type of concrete in practical engineering design and construction has been of great interest to engineers in recent years, since such kind of concrete can reduce the column size, increase the strength-to-weight ratio, flexural stiffness and rigidity, provide a more cost effective solution of structural form of tall buildings and shorten the construction cycle. However, the application of HSC or UHSC on practical construction is very limited. One of the reasons that inhibits the adoption of HSC or UHSC is owing to its brittleness (Kwan 2000). As reported by Pam *et al*. (2001), HSC beams would fail abruptly if the reinforcement ratio was high.

*Corresponding author, Ph.D., E-mail: johnny.ho@uq.edu.au

http://www.techno-press.org/?journal=eas&subpage=7 ISSN: 2092-7614 (Print), 2092-7622 (Online)

Traditionally in the design of reinforced concrete (RC) columns, transverse reinforcement is adopted to confine the concrete core. Results showed that installing the transverse reinforcement will increase the ductility (Pam and Ho 2009) of columns. However, the efficiency of the transverse reinforcement decreases significantly as the concrete strength increases. It implies that in confining HSC or UHSC columns, the required transverse steel may become too congested to allow satisfactory placing quality of concrete (Ho and Pam 2003, Zhou *et al*. 2010), which can easily lead to segregation and honeycombing. More importantly, the transverse reinforcement will only confine the core concrete but not the concrete cover. After reaching the spalling strain, such as during earthquake (Li *et al*. 1991, Mehrparvar and Khoshnoudian 2011), the concrete cover will fall off. Subsequently, the strength and ductility enhancement due to the confining action will decrease owing to the reduction in concrete area and increase in axial load level respectively.

To further push up the maximum deign strength of concrete in column construction, concrete-filled-steel-tube (CFST) column which consists of a hollow steel tube with concrete in-filled is recommended (Giakoumelis and Lam 2004, Han 2004, Zhong 2006, Han *et al*. 2011) to replace traditional confined RC columns. Due to the beneficial composite action, inward buckling of steel tube can be prevented or delayed by the core concrete and the steel tube will in turn provide effective lateral confining pressure to the entire concrete section. This confinement effect will be maximized when adopting circular section since the circular steel tube can provide membrane-type hoop confining stress to the concrete in-filled, while the restraining action for square of rectangular section is mainly due to plate bending (Schneider 1998). Thus, CFST columns show superior strength and ductility performance compared to the conventional reinforced concrete columns (Fam *et al*. 2004, Han 2004, Zhong 2006, Han *et al*. 2011). Furthermore, the increased strength-to-weight ratio can reduce the use of materials and increase the usable area, which leads to a more sustainable environment. This is extremely important for the design and construction of tall buildings in cities like Hong Kong, where the lettable area is so limited. More importantly, such an increase in the strength-to-weight ratio due to the provision of stronger and more uniform confinement will not jeopardise the ductility even adopting HSC or UHSC. Therefore, high-strength concrete-filled-steel-tube (HSCFST) columns are becoming increasing popular to researchers and industry.

However, there is a major shortcoming when adopting CFST columns, which is the imperfect interface bonding between concrete and steel tube during initial elastic stage (Liao *et al*. 2011) because of different dilations of steel and concrete. This imperfect interface bonding is not desirable; since it reduces the confining pressure provided by the steel tube and thus the initial elastic stiffness and strength of CFST columns. For example, Giakoumelis and Lam (2004) reported that the difference in uni-axial strength between bonded and un-bonded HSCFST columns could be up to 14% when the concrete strength reached 100 MPa. Xue *et al*. (2012) indicated that the de-bonding would have adverse effects on the ultimate load and ductility of CFST stub columns and the ultimate load could be reduced by 16.9% for concrete cube strength of 62.5 MPa. The adverse effect by imperfect interface bonding can only be improved when the concrete starts crushing, resulting in much larger lateral dilation and thus activating larger confining pressure. To fully utilise the potential of confining action provided by the hollow steel tube at the initial elastic stage, the use of stiffeners and tie bars were proposed previously (Huang *et al*. 2002, Cai and He 2006, Ho and Lai 2013). However, the installation of such confinement is difficult and may affect the concrete placing quality especially when the column size is small.

Hence, a more practical confining scheme by adopting steel rings is proposed (Ho and Luo 2012, Ho *et al*. 2014, Lai and Ho 2014b) to improve the uni-axial behaviour of the HSCFST columns.

In this paper, a total of 29 HSCFST columns with different cross sectional and material properties consisting of external rings were tested under uni-axial compression. The confining effectiveness of the external rings was studied by the axial load against axial strain (and displacement) curves and the lateral strain against axial strain curves. From the tests, it can be concluded that: (1) The externally confined HSCFST columns had uni-axial strength and elastic stiffness larger than those of unconfined HSCFST columns. (2) Rings could decrease the strength degradation rate of the HSCFST columns. (3) Rings could restrict the lateral dilation of HSCFST columns and maintain intact interface bonding. (4) The failure mode for ring-confined HSCFST columns with thinner steel tube and larger spacing of rings was irregular bulge, which indicated shear failure of concrete core under insufficient confinement. (5) The failure mode for ring-confined HSCFST columns with thicker steel tube or confined by smaller spacing of rings was without obvious shear failure plane, which indicates that concrete is well confined against brittle shear failure. Lastly, an analytical model calculating the uni-axial strength of tested specimens was developed based on the Von-Mises and Mohr-Coulomb failure criteria for steel and in-filled concrete respectively. The validity of this analytical model was verified by comparing the predicted theoretical strength with the experimental strength measured in this study and in other researchers' test results.

2. Experimental programme

The details of specimens, loading machine, test set-up and procedure are briefly summarized below.

2-1 Details of specimens

A total of 29 HSCFST columns with concrete cylinder strength from 75 to 120 MPa and different cross-section properties were fabricated and tested under uni-axial compression (Lai and Ho 2013). The HSCFST columns specimens were divided into 5 groups depending on the sectional properties and concrete strength, as shown in Table 1. In each group, one of the specimens was unconfined (i.e., without external rings), which served as control specimen for comparison purpose. The rest of the specimens were installed with external rings at different spacing, S (i.e., 5t, 10t, 12.5t, 15t and 20t, where t is the thickness of the steel tube). The external steel rings (diameter d = 8 mm and nominal yield strength f_{yr} = 250 MPa) were intermittent welded to the external surface of the steel tube at eight welding spots at each level. The welding spots were evenly distributed around the circumference of the steel tube, which were separated from each other by 45°. An overlapping length of 10 times the diameter was provided to the steel rings to ensure that the yield strength of the ring could be fully developed. Details of the specimens are shown in Fig. 1.

A naming system was established to identify each of the specimens. It consists of two alphabets and four numbers. For example, CR5-5-168-80 represents a HSCFST column specimen

Fig. 1a Photos of HSCFST specimens

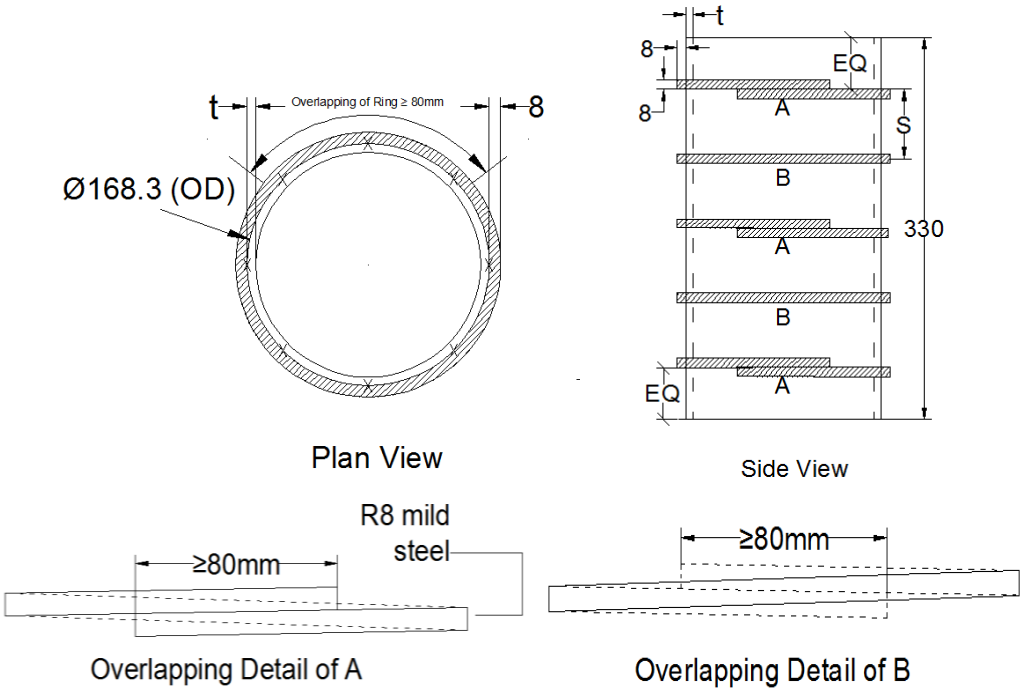

Fig. 1b CFST column – Confined by the external rings

(indicated by the first letter "C") confined by external steel ring (indicated by the second letter "R"). The spacing of the external ring is 5 times the thickness of the steel tube, i.e., 5*t*, (indicated by the first number "5"). The thickness of the steel tube is 5 mm (indicated by the second number "5"). The outer diameter of the steel tube is about 168 mm (indicated by the third number "168") and lastly, the concrete cylinder strength is about 80 MPa on the testing day (indicated by the last number "80"). The HSCFST column without steel rings is represented by CN0-5-168-80, where N0 stands for "no confinement".

Table 2 Strain degradation rate of tested HSCFST columns

Group No.	Specimens	σ_{sy} (MPa)	f_c' (MPa)	Thickness of steel tube, t (mm)	Spacing of rings, S (mm)	N_{exp} (kN)	Strength Ratio	Stiffness (GPa)	Stiffness Ratio
1	CR5-5-168-80	365	85.4	5	25	3643	1.25	57	1.07
	CR10-5-168-80	365	85.4	5	50	3205	1.10	53.6	1.01
	CR12.5-5-168-80	365	85.4	5	62.5	3178	1.09	58.5	1.10
	CR15-5-168-80	365	85.4	5	75	3079	1.05	51	0.96
	CR20-5-168-80	365	85.4	5	100	3149	1.08	57.7	1.09
	CN0-5-168-80	365	85.4	5	-	2926	1.00	53.1	1.00
2	CR5-8-168-80	365	75.2	8	40	3523	1.14	66.5	1.01
	CR10-8-168-80	365	75.2	8	80	3317	1.07	81.6	1.24
	CR12.5-8-168-80	365	85.4	8	100	3600	1.16	71.7	1.09
	CR15-8-168-80	365	75.2	8	120	3218	1.04	77.2	1.17
	CR20-8-168-80	365	75.2	8	160	3171	1.02	71.1	1.08
	CN0-8-168-80	365	75.2	8	-	3101	1.00	65.8	1.00
3	CR5-10-168-90	365	95.1	10	50	4234	1.08	77.7	1.01
	CR10-10-168-90	365	95.1	10	100	4130	1.05	77.1	1.00
	CR12.5-10-168-90	365	95.1	10	125	4285	1.09	76.1	0.99
	CR15-10-168-90	365	95.1	10	150	4361	1.11	78.3	1.02
	CR20-10-168-90	365	95.1	10	200	4063	1.03	74.6	0.97
	CN0-10-168-90	365	95.1	10	-	3930	1.00	76.9	1.00
4	CR5-5-114-120	425	114.3	5	25	2340	1.25	73.4	1.17
	CR10-5-114-120	425	114.3	5	50	2167	1.16	66.4	1.06
	CR12.5-5-114-120	425	114.3	5	62.5	2065	1.10	61.9	0.98
	CR15-5-114-120	425	116.7	5	75	2110	1.13	69.1	1.10
	CR20-5-114-120	425	114.3	5	100	1977	1.05	69	1.10
	CN0-5-114-120	425	114.3	5	-	1875	1.00	62.9	1.00
5	CR5-10-139-120	365	120.0	10	50	3621	1.13	94.7	1.06
	CR10-10-139-120	365	120.0	10	100	3207	1.00	90.4	1.01
	CR15-10-139-120	365	120.0	10	150	3180	0.99	85.5	0.95
	CR20-10-139-120	365	120.0	10	200	3301	1.03	88.6	0.99
	CN0-10-139-120	365	120.0	10	-	3208	1.00	89.7	1.00

2.2 Test set-up and procedure

In this experiment, the SATEC Series RD Model with maximum load of 5,000 kN and maximum travelling displacement of 100 mm was adopted for the test. The details of the test set-up and instrumentations are shown in Fig. 2. Three linear variable differential transducers (LVDTs) with 100 mm stroke were installed to record the axial displacement of the entire HSCFST columns by measuring the relative displacement between the top and bottom loading platens. Three numbers of bi-directional strain gauges (Tokyo Sokki Kenkyujo Co., Ltd) were installed at around the mid-height of the external face of the tested specimens, which were 120° separated from each other to measure the longitudinal and transverse strains. A circumferential extensometer with maximum measuring range of 6 mm was installed at about 8 mm (a ring diameter) from the external rings to measure the tube dilation during the initial elastic stage. The extensometer would be removed when the lateral dilation was about to reach 6 mm. In some specimens, one-directional strain gauges were installed on the surface of the external rings to monitor the strains developed.

All the HSCFST columns were tested under quasi-static incremental displacement with strain control. The top surface was packed with a layer of rapid-hardening gypsum before initial compression was applied so that a smooth contact between the platen, concrete and steel tube can be formed to enable even transfer of applied axial load. Initially, specimens were unloaded to 10 to 20 kN, which is less than 1% of the applied maximum load and, subsequently, the test would start. The initial loading rate for specimens of 330 mm height was 0.3 mm/min and that for 248 mm height was 0.2 mm/min. The loading rate would then increase at a rate of 0.05 mm/min for every 2 mm increase in the axial displacement after reaching 10 mm. The loading application would stop when the axial strain was larger than 0.2, or when the applied load dropped to less than 70% of the measured maximum load, or when the applied load reached 90% of the machine capacity (4500 kN), whichever was the earliest.

Fig. 2a Test set-up

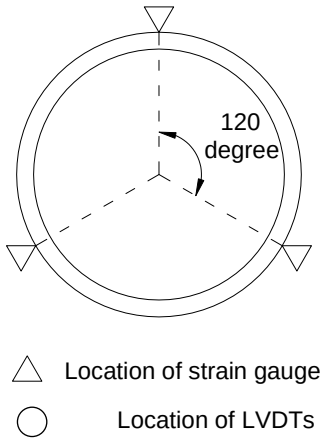

Fig. 2b Instrumentation (Plan view)

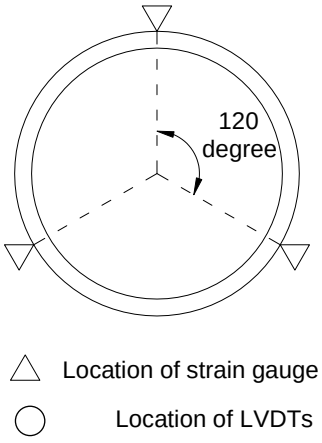

Fig. 2c Instrumentation (Side view)

3. Test results and discussions

3.1 Axial load against axial strain (displacement) curves

The measured axial load is plotted against the axial strain (and displacement) for all the tested HSCFST columns in Fig. 3. The axial load is obtained directly from the machine while the axial strain is obtained by the LVDTs reading adjusted for the axial deformation of the gypsum (Lai and Ho 2014a). It can also be seen from Fig. 3 that initially the axial load increases as the axial strain increases linearly. As the axial strain increases, the Poisson's ratio of core concrete will increase

and be larger than that of steel tube owing to the gradual development of internal micro-cracks. At this stage, the load sharing pattern will change, where the steel tube shares less and the concrete shares more. The curve at the stage would start to change from linear to nonlinear behaviour until the maximum strength was achieved. After reaching the first maximum strength, the axial load drops because of the crushing of the in-filled HSC. Under this circumstance, the axial load capacity of the concrete core dropped rapidly, which decreased the axial load-carrying capacity of the HSCFST columns. When the axial strain increased further, the lateral dilation of core concrete increased quickly that activated larger confining pressure provided by the external rings. Since the dilation of concrete and the confining pressure increased rapidly afterwards, this offset the strength degradation due to the formation of micro-cracks in the core concrete. Interestingly, as the spacing of rings decreased, the ultimate strength of the HSCFST columns increased and the shape of the descending branch after peak strength became smoother. This is because as the ring spacing reduced, the confinement effect increased, which provided larger and more uniform confining pressure to the core concrete. It then improves the strength and ductility performances of the core concrete and thus the columns. If the ring spacing was decreased to the minimum of 5t in this study (i.e., CR5-8-168-80 and CR5-10-168-90), no strength degradation was observed.

To study the effectiveness of confinement due to the provision of external rings, the maximum axial load-carrying capacity, N_{exp} and the initial elastic stiffness for all HSCFST specimens were recorded in order to study their enhancement. The obtained values of the load-carrying capacities, N_{exp}, which is defined as the maximum load measured at the first peak point on the axial strength against axial strain (displacement) curves (See Fig. 3), are listed in Table 1. For specimens CR5-8-168-80 and CR5-10-168-90, which present strain hardening behaviour (i.e., strength increases monotonically as displacement increases), the ultimate load is defined as strength at 1% strain, which is close to strain at first peak of other tested specimens. On the other hand, the elastic stiffness is calculated from the initial slope of the graph and divided by the total area of the specimens, which are also listed in Table 1.

To study the effects of adding steel rings on the improvement of axial load-carrying capacity and elastic stiffness, the strength (or stiffness) enhancement ratio, defined as the ratio of the strength (or stiffness) of the ring-confined HSCFST columns to the respective value of the unconfined HSCFST columns, has been adopted. The so obtained enhancement is summarised in Table 1. It is evident from the table that the addition of external steel rings can improve the axial load-carrying capacity and elastic stiffness on average by 9.1% and 5.1% respectively. On the other hand, the maximum load-carrying capacity and elastic improvement obtained in this study is 24.8% and 24.0% respectively.

The beneficial effect on the deformation of HSCFST columns due to ring provision was also studied by the strain degradation rate $\mu_{95\%}$ defined as follows:

$$\mu_{95\%} = -\frac{N_{95\%} - N_{exp}}{\varepsilon_{95\%} - \varepsilon_u} \tag{1}$$

where $N_{95\%}$ is the strength at 95% of the ultimate strength N_{exp} after reaching N_{exp}. $\varepsilon_{95\%}$ and ε_u are the strains corresponding to $N_{95\%}$ and N_{exp} respectively.

The strain degradation rates for all the HSCFST columns are tabulated in Table 2. It is apparent that the ultimate strain ε_u for confined HSCFST columns is larger than that of the unconfined counterpart, which indicates that the ring-confined specimens will have larger strain to mobilize the axial strength. Thus, the ultimate strength for ring-confined specimens is higher. It can be verified experimentally by comparing the obtained N_{exp} with ε_u for CR10-10-139-120,

Table 2 Strain degradation rate of tested HSCFST columns

Group no.	Specimens	N_{exp} (kN)	ε_u (με)	$N_{95\%}$ (kN)	$\varepsilon_{95\%}$ (με)	$\mu_{95\%}$
1	CR5-5-168-80	3643	12212	3461	21242	20.17
	CR10-5-168-80	3205	7475	3045	14212	23.79
	CR12.5-5-168-80	3178	6193	3019	10150	40.16
	CR15-5-168-80	3079	6167	2925	9346	48.43
	CR20-5-168-80	3149	5664	2992	11125	28.83
	CN0-5-168-80	2926	4978	2780	6261	114.03
2	CR5-8-168-80	3523	10094	3347	*	*
	CR10-8-168-80	3317	8869	3151	-	-
	CR12.5-8-168-80	3600	8505	3420	10955	73.47
	CR15-8-168-80	3218	10112	3057	-	-
	CR20-8-168-80	3171	5705	3012	13748	19.71
	CN0-8-168-80	3101	6720	2946	12751	25.71
3	CR5-10-168-90	4234	10000	4022	*	*
	CR10-10-168-90	4130	8877	3924	-	-
	CR12.5-10-168-90	4285	8503	4071	-	-
	CR15-10-168-90	4361	7207	4143	-	-
	CR20-10-168-90	4063	10600	3860	-	-
	CN0-10-168-90	3930	8393	3734	-	-
4	CR5-5-114-120	2340	13533	2223	-	-
	CR10-5-114-120	2167	11871	2059	22738	9.97
	CR12.5-5-114-120	2065	7737	1962	10378	39.10
	CR15-5-114-120	2110	7316	2005	10961	28.94
	CR20-5-114-120	1977	6157	1878	10370	23.46
	CN0-5-114-120	1875	5531	1781	8353	33.22
5	CR5-10-139-120	3621	11530	3440	-	-
	CR10-10-139-120	3207	7333	3047	10909	44.84
	CR15-10-139-120	3180	6824	3021	10350	45.09
	CR20-10-139-120	3301	8708	3136	-	-
	CN0-10-139-120	3208	7884	3048	10864	53.83

Remarks:

*: Specimens show strain hardening behaviour and no strength degradation rate is presented

-: The load-carrying capacity of HSCFST columns is always higher than 95% of the ultimate load after the slightly drop in the first peak point.

The above specimens can be regarded as having no strength degradation

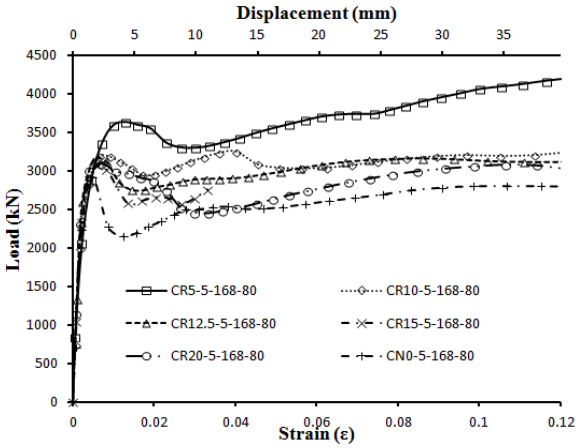

Fig. 3a Axial load against axial strain (displacement) curves (Group no. 1)

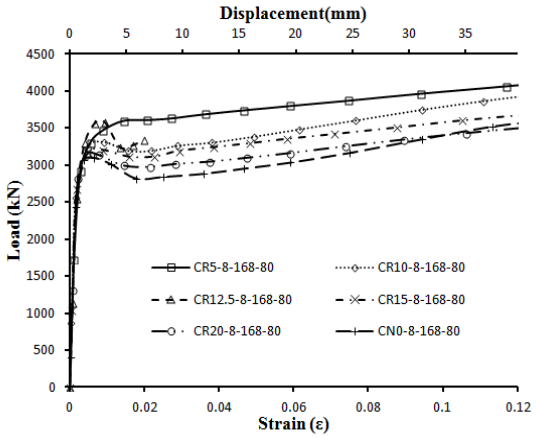

Fig. 3b Axial load against axial strain (displacement) curves (Group no. 2)

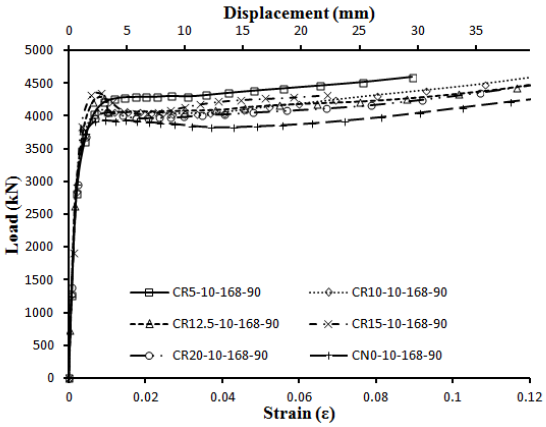

Fig. 3c Axial load against axial strain (displacement) curves (Group no. 3)

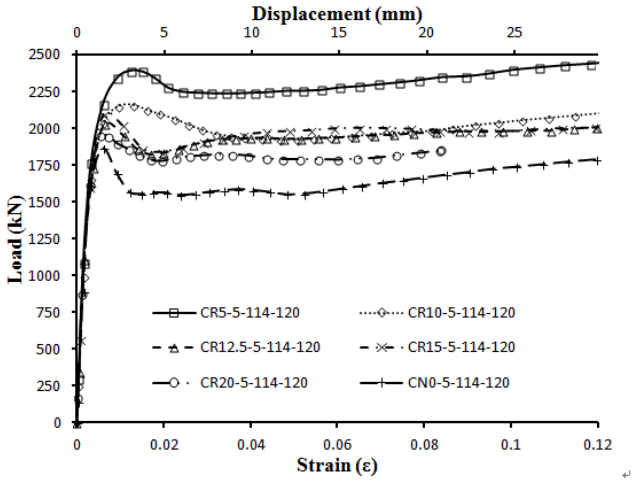

Fig. 3d Axial load against axial strain (displacement) curves (Group no. 4)

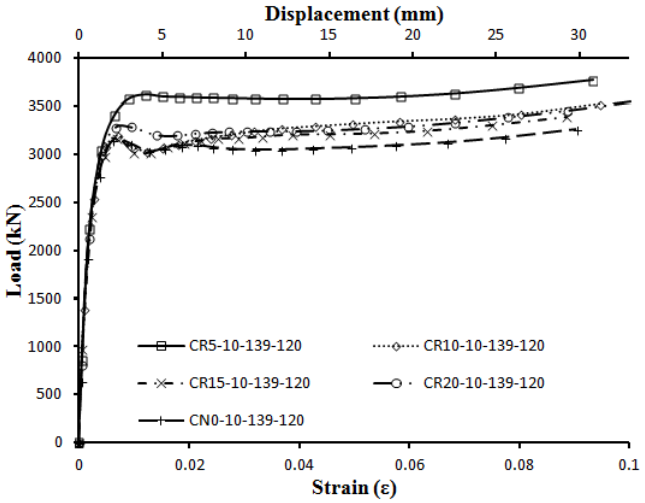

Fig. 3e Axial load against axial strain (displacement) curves (Group no. 5)

CR15-10-139-120 and CR20-10-139-120. It can also be observed from Table 2 that, the strain degradation rate $\mu_{95\%}$ of the unconfined HSCFST columns is larger than that of the ring-confined specimens. This shows that the rings did improve the ductility and deformability of the HSCFST. For specimens with thick steel tube and small spacing of rings, since the confinement effect provided by the steel tube and rings is sufficient to compensate the loss of strength due to crushed concrete, the strain degradation in the post-peak region would not be shown (i.e., CR5-8-168-80 and CR5-10-168-90). For these two specimens, the values of $\mu_{95\%}$ are not presented and marked with "*" in Table 2; For specimens CR10-8-168-80, CR15-8-168-80, CR5-5-114-120, CR5-10-139-120, CR20-10-139-120 and those in Group 3 other than CR5-10-168-90, the load-carrying capacity is always higher than 95% of the ultimate load after the slightly drop in the first peak point. For these specimens, the values of $\mu_{95\%}$ are marked with "-" in the same table.

3.2 Axial strain against lateral strain curves

The effectiveness of providing external rings to improve the interface bonding can be studied by investigating the variation of lateral strain against longitudinal strain. Three different methods are adopted in this study to measure the lateral strain developed in columns under uni-axial compression. Method LS1 is to measure the lateral strain developed on the steel rings by some uni-directional strain gauges installed on them. Method LS2 is to measure the average lateral strain by the average expansion of the column circumference using circumferential extensometers. Method LS3 is to measure the average localised lateral strain on the hollow steel tube by three bi-directional strain gauges installed on the exterior surface of steel tube. Typical variation of the measured lateral strains by the above three methods for some specimens are plotted against the longitudinal strain in Fig. 4. The slopes of the initial straight line portion of these graphs (i.e., for longitudinal strain smaller than 1600 με), which are the Poisson's ratio of the specimens, are evaluated and presented in Fig. 4 and Table 3.

The measured lateral strains plotted in Fig. 4 for LS1 were taken as the largest recorded strain values by all the strain gauges installed on rings, whereas those for LS3 were taken as the average strain values recorded by the three bi-directional strain gauges. On the other hand, the plotted lateral strains for LS2 as shown in Fig. 4 were obtained by dividing the circumferential expansion (measured by the circumferential extensometer) by the circumference of the steel tube. The axial strains were obtained by the adjusted LVDTs reading to take into account any possible deformation in the gypsum under compression (Lai and Ho 2014a).

From Table 3 and Fig. 4, it can be seen that Poisson's ratios of the confined HSCFST columns obtained from LS1 are smaller than the typical Poisson's ratio of concrete (~0.2). The Poisson ratios obtained from LS2 are mostly between 0.184 and 0.252 with an average value of about 0.224, which is smaller than that of steel tube (~0.3). Nevertheless, the obtained Poisson'sratios of the columns in LS3 are similar to that of steel tube because the strain gauges were installed at localised areas mid-way between rings, at which the least confining pressure was provided. Consequently, the steel tube would bend slightly outward between the rings during uni

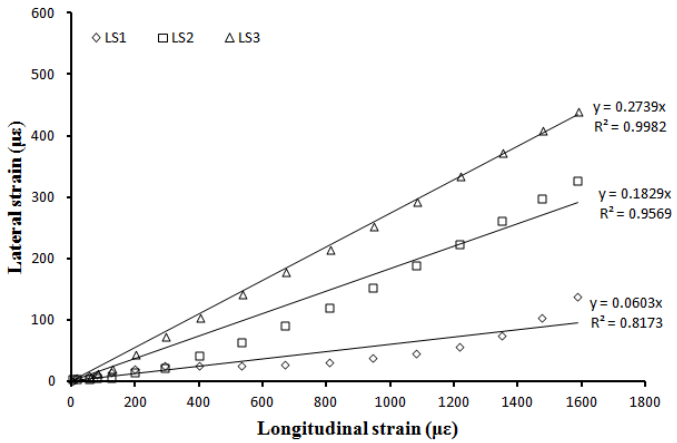

Fig. 4a Lateral strain against longitudinal strain curves (CR15-5-168-80)

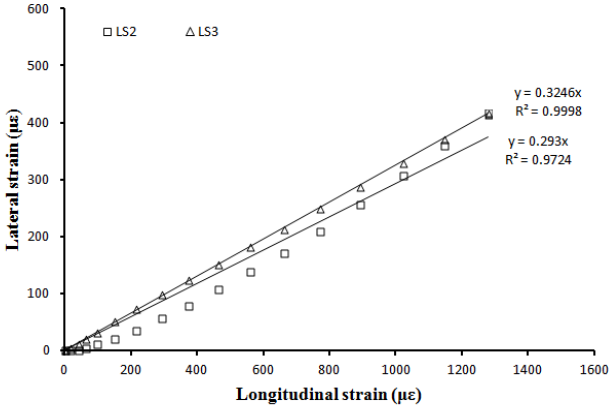

Fig. 4b Lateral strain against longitudinal strain curves (CR15-8-168-80)

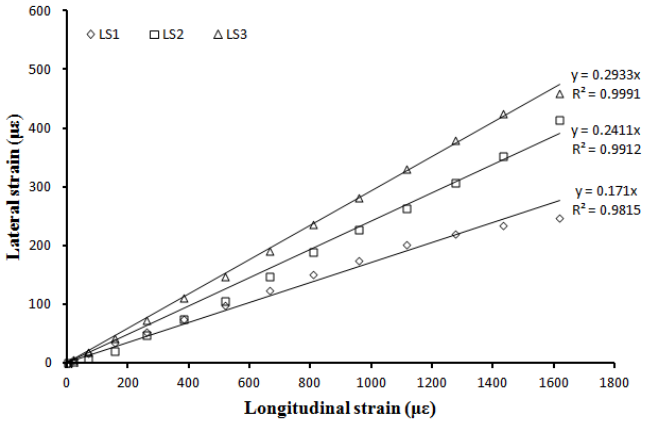

Fig. 4c Lateral strain against longitudinal strain curves (CR15-10-168-90)

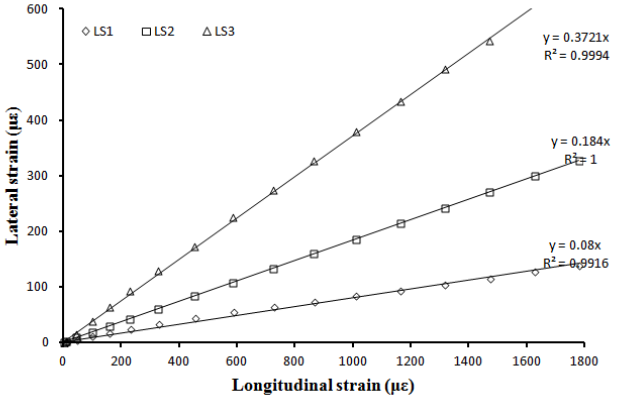

Fig. 4d Lateral strain against longitudinal strain curves (CR15-5-114-120)

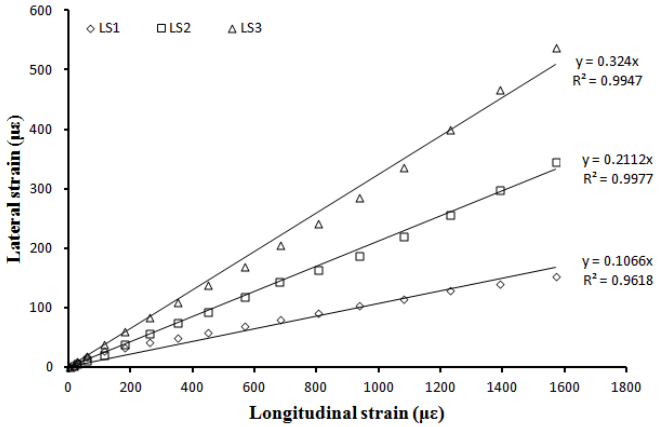

Fig. 4e Lateral strain against longitudinal strain curves (CR15-10-139-120)

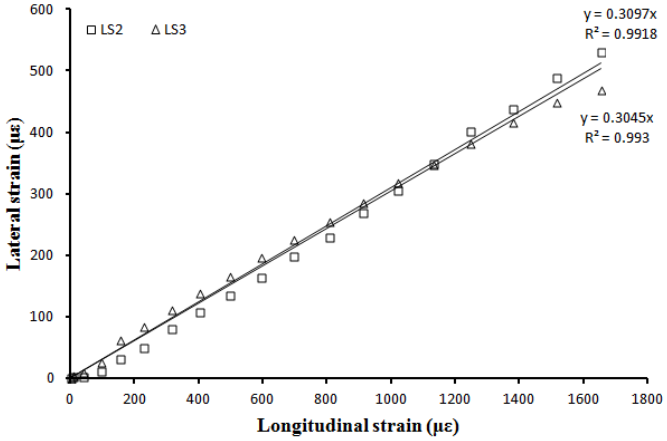

Fig. 4f Lateral strain against longitudinal strain curves (CN0-10-168-90)

Fig. 5a Failure mode of HSCFST columns (Group no. 1)

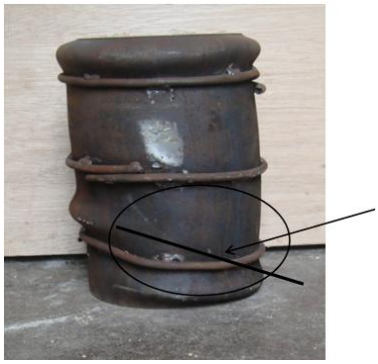

Fig. 5b Failure mode of HSCFST columns (CR20-5-168-80)

Fig. 5c Failure mode of HSCFST columns (Group no. 3)

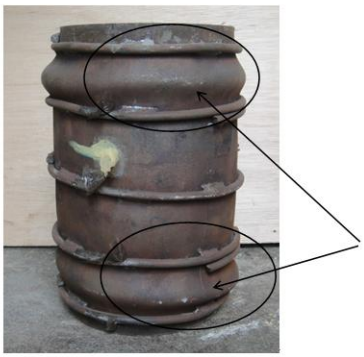

Fig. 5d Failure modes of ring-confined HSCFST columns

Fig. 5e Failure modes of unconfined HSCFST columns

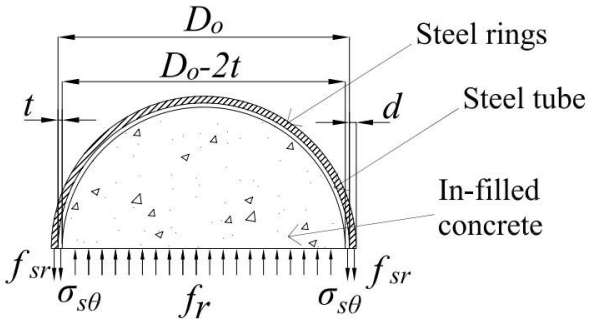

Remark: The overall height of specimen is *H*

Fig. 6 Free body diagram for ring-confined HSCFST columns

Table 3 Poisson's ratio

Group No.	Specimens	LS1	LS2	LS3
1	CR5-5-168-80	-	-	0.245
	CR10-5-168-80	0.221	-	0.331
	CR12.5-5-168-80	-	0.261	0.288
	CR15-5-168-80	0.060	0.183	0.274
	CR20-5-168-80	-	0.199	0.281
	CN0-5-168-80	-	0.318	0.297
2	CR5-8-168-80	-	0.285	0.277
	CR10-8-168-80	-	0.159	0.311
	CR12.5-8-168-80	-	0.189	0.269
	CR15-8-168-80	-	0.293	0.325
	CR20-8-168-80	-	0.277	0.291
	CN0-8-168-80	-	0.328	0.308
3	CR5-10-168-90	0.215	0.241	0.296
	CR10-10-168-90	0.101	0.204	0.312
	CR12.5-10-168-90	0.120	0.252	0.313
	CR15-10-168-90	0.171	0.241	0.293
	CR20-10-168-90	0.195	0.243	0.317
	CN0-10-168-90	-	0.305	0.310
4	CR5-5-114-120	0.107	-	0.293
	CR10-5-114-120	0.221	0.224	0.321
	CR12.5-5-114-120	0.120	0.193	0.304
	CR15-5-114-120	0.080	0.184	0.375
	CR20-5-114-120	0.103	0.195	0.326
	CN0-5-114-120	-	0.255	0.270
5	CR5-10-139-120	0.134	0.233	0.327
	CR10-10-139-120	0.068	0.236	0.307
	CR15-10-139-120	0.107	0.211	0.324
	CR20-10-139-120	0.139	0.203	0.352
	CN0-10-139-120	-	0.293	0.307

Remarks:

-: Strain gauges / extensometers were not installed

-axial compression, as shown in the failure photos in Fig. 5 later. For the unconfined columns, the Poisson's ratios obtained from LS2 and LS3 are similar, which are approximately equal to the Poisson's ratio of the steel tube. From the above comparison, it can be concluded that the interface bonding condition has been improved by the external rings, which restrict effectively the lateral dilation of the steel tube. In particular, perfect interface bonding condition can be achieved at, or close to, the locations of rings.

3.3 Failure modes

Generally speaking, the failure mode for all the HSCFST columns was local buckling. More specifically, the failure of HSCFST columns was due to outward folding of steel tube pushed by the in-filled concrete (See Figs. 5a and 5b). From Figure 5b, it can be seen that shear failure plane occurred among the bulges for HSCFST columns with thin steel tube and large spacing of rings. This is because in this kind of specimens, the confinement effect provided by the steel tube and rings was not sufficient to prevent concrete shear cracks from propagating, and thus caused irregular bulges. For HSCFST columns with thick steel tube or confined by smaller ring spacing, such as those in Group no. 3, there is no obvious shear failure plane along the height and the buckling mode was uniform bulges as shown in Fig. 5c. Again, it proves that HSC or UHSC can be effectively confined by hollow steel tube with adequate tube thickness and provided with external steel rings.

From the load-displacement curve shown in Fig. 3, it is apparent that the strength and ductility increases when the HSCFST columns are provided with rings. This can be explained by the fact that the failure mode of ring-confined HSCFST columns was the local buckling between rings, which provided effective lateral restraints to the steel tube, as shown in Fig. 5d. Accordingly, the in-filled concrete was provided with larger and more uniform confining pressure, and improved in both strength and ductility. Conversely, from Fig. 5e, it could be observed that buckling occurred earlier in unconfined HSCFST columns owing to the longer effective length and the local buckling due to end effect close to the top and bottom loading platens. The confining pressure that can be provided to the concrete at failure was hence smaller and thereby reducing the load-carrying capacity and ductility of HSCFST columns.

4. Proposed model for load-carrying capacity

An analytical model is proposed in this section for calculating the uni-axial strength of HSCFST columns. This model takes into account the confinement effect provided by the steel tube and external steel rings. The model evaluates the axial load-carrying capacity of HSCFST columns by summing up the capacity of steel tube and core concrete considering force equilibrium condition. In this model, the steel tube is assumed to follow the Von-Mises failure criterion and core concrete to follow Mohr-Coulomb failure criterion.

4.1 Proposed model

By ignoring the radial stress of steel tube, the hoop stress $\sigma_{s\theta}$ and longitudinal stress σ_{sz} at failure can be related to the uni-axial yield strength of the steel tube by the Von-Mises failure criterion as shown in Eq. (2):

$$\sigma_{s\theta}^2 + \sigma_{s\theta}\sigma_{sz} + \sigma_{sz}^2 = \sigma_{sy} \quad (2)$$

Since concrete is a non-ductile material, Von-mises failure criterion is not applicable. In this study, the Mohr-Coulomb failure criterion, as shown in Eq. (3), has been adopted to model the concrete behaviour:

$$f_{cc} = \frac{1+sin\varphi}{1-sin\varphi} f_r + 2c\frac{cos\varphi}{1-sin\varphi} \quad (3)$$

where f_{cc} is the confined concrete stress; f_r is the confining pressure; c and φ are the cohesion and internal friction angle of concrete at failure, respectively. In particular under the uni-axial stress state (f_r = 0), we have the following boundary condition:

$$f_{cc} = 2c\frac{cos\varphi}{1-sin\varphi} = f_c' \quad (4)$$

where f_c' is the unconfined concrete strength. Thus, Eq. (3) becomes:

$$f_{cc} = \frac{1+sin\varphi}{1-sin\varphi} f_r + f_c' = kf_r + f_c' \quad (5)$$

where k is the coefficient related to the internal friction angle φ.

Richart *et al*. (1929) suggested that k can be taken as approximately equal to 4. Cai (2003) recommended that k should vary with confining pressure f_r. By carrying out a series of tri-axial tests, Hawkins (1968) figured out that the internal friction angle φ of concrete changed from about 50° to 30°. It was found that the internal friction angle increases as the confining pressure decreases, and k for concrete should vary from 3.00 to 7.55. In this study, the effects on f_{cc} due to variation in the steel tube thickness, spacing of steel rings, concrete strength and steel yield strength have been taken into account and are eventually reflected in the value of k and φ.

For HSCFST columns confined with large confining pressure, the internal friction will be smaller. Accordingly, the value of k decreases. On the other hand, as the concrete strength increases, the elastic modulus of concrete also increases that decreases the concrete lateral expansion and hence confining pressure. Thus, the value of k increases as concrete strength f_c' increases. As of the effect of the steel tube yield strength σ_{sy}, k decreases as σ_{sy} increases, which improve the confining pressure provided to the concrete. From the above discussion, it is evident that the value of k is solely influenced by a single parameter named the confinement index ξ_t, which can be expressed in terms of the strength and geometry of concrete and steel. The confinement index is defined in Eq. (6) as the ratio of the steel capacity (rings included) to concrete capacity:

$$\xi_t = \frac{A_{st}\sigma_{sy}}{A_c f_c'} \quad (6)$$

$$A_{st} = A_s + \frac{\pi}{4}\frac{d^2\pi D_o}{S}\frac{f_{yr}}{\sigma_{sy}} \quad (7)$$

where A_{st}, A_s and A_c are the equivalent total steel area (incorporated the external steel ring as the part of the steel tube thickness), steel tube cross-sectional area and concrete cross-sectional area, respectively; D_o is the outer diameter of the steel tube; d is the diameter of rings; f_{yr} is the yield strength of steel rings.

Having defined the confinement index, the relationship between k (or φ) with ξ_t is then developed. As discussed above, shear failure of concrete occurs in HSCFST columns with thinner steel tube and larger spacing of rings. Previously, Han (2007) concluded that for circular CFST columns, strain hardening behaviour (i.e., columns do not show strength degradation in the post-

peak region) would occur when the confinement index is larger than 1.12, which was also named critical confinement index ξ_{cr}. However, Han did not consider the effect of concrete strength, which was shown in the authors' past research (Lai and Ho 2014b) that significantly influenced the ξ_{cr}. For higher strength concrete, larger confining pressure is needed to confine the concrete than that in lower strength concrete because the brittleness of concrete increases. Thus, the critical confinement index ξ_{cr} should increases as concrete strength increases, until a maximum value of ξ_{cr} = 1.19 is reached (Lai and Ho 2014b). The empirical equations correlating ξ_{cr} and f_c' are rewritten as follows:

$$\xi_{cr} = \begin{cases} 0.61 & f_c' \in (0,25] \\ 0.0116 f_c' + 0.32 & f_c' \in (25,75] \\ 1.19 & f_c' \in (75,120] \end{cases} \tag{8}$$

Eq. (8) matches with those indices of the specimens, which exhibit strain hardening behaviour in this study (e.g. CR5-8-168-80 and CR5-10-168-90). It means that for CFST columns with confinement index larger than or equal to ξ_{cr} (in this case 1.19), the confinement effect provided by the steel tube is large enough to prevent the shear failure of the in-filled concrete that should be adopted in the design of CFST columns normally. Nevertheless, this condition cannot be easily fulfilled in practical design of HSCFST columns because it will need a very thick steel tube that may not be practicable or economical. Therefore in designing HSCFST columns, strain hardening is not always practically achievable and design formulas will be needed to cover the design with $\xi_t < \xi_{cr}$.

In the case where strain hardening occurs (i.e., $\xi_t \geqslant \xi_{cr}$), shear failure is unlikely to happen and the minimum value of φ = 30° proposed by Hawkins is adopted. On the other hand, in the case of unconfined concrete where ξ_t = 0, the maximum value of φ = 50° proposed by Hawkins is adopted. The intermediate values of φ for $0 < \xi_t < \xi_{cr}$ are assumed to vary linearly between 50° and 30°. The entire equation is shown as follows:

$$\varphi = \begin{cases} 50° & \xi_t = 0 \\ 50° - \frac{20°}{\xi_{cr}}\xi_t & 0 < \xi_t < \xi_{cr} \\ 30° & \xi_t \geq \xi_{cr} \end{cases} \tag{9}$$

The confining pressure f_r can be expressed in the following form by considering the free body diagram using force equilibrium equation as shown in Fig. 6.

$$f_r(D_o - 2t)H = 2\sigma_{s\theta} tH + 2f_{sr}\frac{\pi}{4}d^2 n \tag{10}$$

$$f_{sr} = E_{sr}\varepsilon_{sr} \leq f_{yr} \tag{11}$$

where H is the overall height of HSCFST columns; t is the thickness of the steel tube; f_{sr}, ε_{sr} and E_{sr} are respectively the stress, strain and elastic modulus of steel rings; n is the number of rings.

Based on the strain gauges readings on the steel rings, it can be concluded that the steel rings yield when the HSCFST columns achieve the ultimate strength. Therefore, Eq. (10) becomes:

$$f_r = \frac{2\sigma_{s\theta} tH + 2f_{yr}\frac{\pi}{4}d^2 n}{(D_o - 2t)H} \approx \frac{2t}{D_o - 2t}\sigma_{s\theta} + \frac{\pi d^2}{2(D_o - 2t)S} f_{yr} \tag{12}$$

where S is the spacing of external rings and S ranged from 5t to 20t (t is the thickness of steel tube, 5, 8 and 10 mm); d is equal to 8 mm. For the hoop stress $\sigma_{s\theta}$, the following equation was established from the test results:

Table 4 Test results and predicted results of HSCFST columns (Authors' results)

Group No.	Specimens	Confinement index ξ_t	k	N_{exp} (kN)	N_{pre} (kN)	N_{exp}/N_{pre}
1	CR5-5-168-80	0.72	4.20	3643	3434	1.06
	CR10-5-168-80	0.64	4.46	3205	3203	1.00
	CR12.5-5-168-80	0.62	4.51	3178	3153	1.01
	CR15-5-168-80	0.61	4.55	3079	3119	0.99
	CR20-5-168-80	0.60	4.59	3149	3075	1.02
	CN0-5-168-80	0.56	4.74	2926	2939	1.00
2	CR5-8-168-80	1.19	3.00	3523	3379	1.04
	CR10-8-168-80	1.13	3.12	3317	3286	1.01
	CR12.5-8-168-80	0.99	3.45	3600	3498	1.03
	CR15-8-168-80	1.11	3.16	3218	3253	0.99
	CR20-8-168-80	1.10	3.18	3171	3236	0.98
	CN0-8-168-80	1.07	3.25	3101	3185	0.97
3	CR5-10-168-90	1.19	3.01	4234	4012	1.06
	CR10-10-168-90	1.15	3.09	4130	3940	1.05
	CR12.5-10-168-90	1.14	3.11	4285	3925	1.09
	CR15-10-168-90	1.13	3.12	4361	3915	1.11
	CR20-10-168-90	1.13	3.14	4063	3902	1.04
	CN0-10-168-90	1.11	3.18	3930	3863	1.02
4	CR5-5-114-120	0.93	3.59	2340	2193	1.07
	CR10-5-114-120	0.84	3.83	2167	2069	1.05
	CR12.5-5-114-120	0.82	3.89	2065	2042	1.01
	CR15-5-114-120	0.79	3.97	2110	2047	1.03
	CR20-5-114-120	0.79	3.96	1977	1999	0.99
	CN0-5-114-120	0.75	4.10	1875	1924	0.97
5	CR5-10-139-120	1.18	3.01	3621	3283	1.10
	CR10-10-139-120	1.14	3.10	3207	3224	0.99
	CR15-10-139-120	1.13	3.13	3180	3204	0.99
	CR20-10-139-120	1.12	3.14	3301	3194	1.03
	CN0-10-139-120	1.10	3.19	3208	3162	1.01
Maximum value						1.11
Minimum value						0.97
Average value						1.03
Standard deviation						0.0377

Table 5 Test results and predicted results of HSCFST columns (Other researchers' results)

Specimens	Confinement index ξ_t	k	N_{exp} (kN)	N_{pre} (kN)	N_{exp}/N_{pre}	References
CA1-1	0.55	4.69	312	305	1.02	Han *et al*. (2005)
CA1-2	0.55	4.69	320	305	1.05	
CA3-1	0.21	6.25	1701	1541	1.10	
CA3-2	0.21	6.25	1670	1541	1.08	
CA4-1	0.15	6.55	2783	2618	1.06	
CA4-2	0.15	6.55	2824	2618	1.08	
CA5-1	0.12	6.74	3950	3974	0.99	
CA5-2	0.12	6.74	4102	3974	1.03	
CB2-1	0.48	4.93	930	851	1.09	
CB2-2	0.48	4.93	920	851	1.08	
CB3-1	0.32	5.68	1870	1713	1.09	
CB3-2	0.32	5.68	1743	1713	1.02	
CB4-1	0.23	6.09	3020	2854	1.06	
CB4-2	0.23	6.09	3011	2854	1.06	
CB5-1	0.19	6.36	4442	4273	1.04	
CB5-2	0.19	6.36	4550	4273	1.06	
CC2-2	0.30	5.82	1910	1785	1.07	
CC3-1	0.18	6.46	4720	4471	1.06	
CC3-2	0.18	6.46	4800	4471	1.07	
S30CS80A	0.33	5.69	2295	2330	0.98	O'Shea and Bridge (2000)
S20CS80B	0.14	6.63	2592	2457	1.06	
S16CS80A	0.13	6.75	2602	2601	1.00	
S12CS80A	0.06	7.18	2295	2403	0.96	
S30CS10A	0.24	6.10	2673	2894	0.92	
S20CS10A	0.10	6.90	3360	3366	1.00	
S12CS10A	0.04	7.27	3058	3173	0.96	
SFE1	0.89	3.44	2180	2388	0.91	Jahansson (2002)
SFE2	0.89	3.44	2170	2388	0.91	
SFE3	0.89	3.44	2190	2388	0.92	
SFE7	0.58	4.66	2740	2899	0.95	
SFE8	0.84	3.83	3220	3232	1.00	
SFE9	1.17	3.05	3710	3434	1.08	

Table 5 Continued

Specimens	Confinement index ξt	k	N_{exp} (kN)	N_{pre} (kN)	N_{exp}/N_{pre}	References
CC4-A-8	0.34	5.64	1781	1822	0.98	Sakino *et al*. (2004)
CC6-A-8	1.25	3.00	2100	1950	1.08	
CC6-C-8	0.53	4.83	5578	5456	1.02	
CC6-D-8	0.32	5.71	11505	11964	0.96	
CC8-A-8	3.22	3.00	2713	2874	0.94	
CC8-C-8	1.40	3.00	7304	7202	1.01	
CC8-D-8	0.79	3.98	13776	14219	0.97	
GH1-1	0.08	7.03	1275	1286	0.99	Tan (2006)
GH1-2	0.08	7.03	1239	1286	0.96	
GH2-1	0.18	6.46	1491	1445	1.03	
GH2-2	0.18	6.46	1339	1445	0.93	
GH3-1	0.41	5.30	1995	1901	1.05	
GH3-2	0.41	5.30	1991	1901	1.05	
GH3-3	0.41	5.30	1962	1901	1.03	
GH4-1	0.57	4.68	2273	2058	1.10	
GH4-2	0.57	4.68	2158	2058	1.05	
GH4-3	0.57	4.68	2253	2058	1.09	
Maximum value					1.10	
Minimum value					0.91	
Average value					1.02	
Standard deviation					0.0565	

$$\frac{\sigma_{s\theta}}{\sigma_{sy}} = (0.15 + 0.09\xi_t)\sigma_{sy} \leq 1.0 \tag{13}$$

Lastly, the ultimate strength of HSCFST columns N_{pre} can be calculated by summing up the strength contributed by in-filled concrete and steel tube:

$$N_{pre} = \sigma_{sz}A_s + f_{cc}A_c \tag{14}$$

4.2 Comparisons with experimental results

To verify the applicability of the proposed formulas (i.e., Eq. (2) to (14)) on predicting the uni-axial strength of ring-confined HSCFST columns, the theoretical results as calculated from the proposed model are compared with the experimental results obtain by other researchers (O'Shea and Bridge 2000, Johansson 2002, Sakino et al. 2004, Han et al. 2005, Tan 2006) on HSCFST columns. The details of comparison are summarised in Table 4 for the authors' tested specimens,

and in Table 5 for the experimental results obtained by other researchers. It is apparent from the Table 4 that the theoretical model can predict fairly accurately the uni-axial strength of HSCFST columns. The ratios between the experimental to theoretical strength vary narrowly within 0.97 to 1.11. The standard deviation obtained is 0.0377. By comparing with the experimental results obtained by other researchers, it can be seen from Table 5 that the theoretical model can predict fairly accurately the uni-axial strength of HSCFST columns. The ratios between the experimental to theoretical strength vary within 0.91 to 1.10. The standard deviation obtained is 0.0565. Thus, the model is applicable in predicting the uni-axial strength of unconfined and ring-confined HSCFST columns for practical design purpose.

5. Conclusions

External steel rings were proposed in this paper to improve the uni-axial behaviour of HSCFST columns. A total of 29 HSCFST columns with and without external rings were tested under uni-axial compression. The effectiveness of adopting external rings on improving the un-axial behaviour of HSCFST columns, such as load-carrying capacity, elastic stiffness, Poisson's ratio, condition of interface bonding and strength degradation was investigated by the axial load against axial strain (displacement) curves and the lateral strain against axial strain curves. From the tested results obtained, it can be concluded that:

(1) External steel rings effectively improve the axial load-carrying capacity of HSCFST columns (Maximum, 24.8%; average, 9.1%). The strength increases as the spacing of rings decreases.

(2) External steel rings effectively improve the elastic stiffness (Maximum 24.0%; average, 5.1%) of HSCFST columns.

(3) For the ring-confined HSCFST columns, the strain degradation rate is always smaller than that of the unconfined counterparts. Thus, external steel rings effectively improve the deformation behaviour of HSCFST columns.

(4) External steel rings are effective since they can limit the lateral deformation of the core concrete and the steel tube, especially at the locations of rings. However, at the locations furthest away from the plane of effective confinement, the confining effect is reduced.

(5) The failure mode for ring-confined HSCFST columns with thinner steel tube and larger spacing of rings is irregular steel tube bulging that indicates shear failure of concrete core under insufficient confinement. However, for HSCFST columns with thicker steel tube or confined by smaller spacing of rings, ther no shear failure plane along the height observed.

(6) For unconfined HSCFST columns, the local buckling was due to the "end effect". For the ring confined HSCFST columns, buckling always occurred between two adjacent rows of the steel rings

An analytical model calculating the uni-axial strength of tested specimens was proposed based on the Von-Mises and Mohr-Coulomb failure criteria for steel and in-filled concrete respectively. The validity of this analytical model is verified by comparing the predicted theoretical strength with the experimental strength measured in this study and in studies conducted by other researchers.

Acknowledgements

The work described in this paper has been substantially supported by a grant from the Research Grants Council of the Hong Kong Special Administrative Region, China (Project No. HKU 712310E). Technical supports for the experimental tests provided by the laboratory staff of the Department of Civil Engineering, The University of Hong Kong, are gratefully acknowledged.

References

Cai, J. and He, Z.Q. (2006), "Axial load behavior of square cft stub column with binding bars", *J. Construct. Steel Res.*, **62**(5), 472-483.

Cai, S.H. (2003), Modern steel tube confined concrete structures, China Communications Press, Beijing, China (in Chinese).

Fam, A., Qie, F.S. and Rizkalla, S. (2004), "Concrete-filled steel tubes subjected to axial compression and lateral cyclic loads", *J. Struct. Eng.*, **130**(4), 631-640.

Giakoumelis, G. and Lam, D. (2004), "Axial capacity of circular concrete-filled tube columns", *J. Construct. Steel Res.*, **60**(7), 1049-1068.

Han, L.H. (2004), "Flexural behaviour of concrete-filled steel tubes", *J. Construct. Steel Res.*, **60**(2), 313-337.

Han, L.H. (2007), "Concrete filled steel structures: Theory and practice (second edition)", Science Press, Beijing, China (in Chinese).

Han, L.H., He, S.H. and Liao, F.Y. (2011), "Performance and calculations of concrete filled steel tubes (cfst) under axial tension", *J. Construct. Steel Res.*, **67**(11), 1699-1709.

Han, L.H., Yao, G.H. and Zhao, X.L. (2005), "Tests and calculations for hollow structural steel (HSS) stub columns filled with self-consolidating concrete (scc)" *J. Construct. Steel Res.*, **61**(9), 1241-1269.

Hawkins, N.M. (1968), "The bearing strength of concrete loaded through rigid plates", *Mag. Concrete Res.*, **20**(62), 31-40.

Ho, J.C.M. and Lai, M.H. (2013), "Behaviour of uni-axially loaded CFST columns confined by tie bars", *J. Construct. Steel Res.*, **83**, 37-50.

Ho, J.C.M., Lai, M.H. and Luo, L. (2014), "Uni-axial behaviour of confined high-strength CFST columns", *Proceedings of the Institution of Civil Engineers. Structures and buildings*, 166(SB1), 1-14.

Ho, J.C.M. and Luo, L. (2012), "Uni-axial behaviour of normal-strength concrete-filled-steel-tube columns with external confinement", *Earthq. Struct.*, **3**(6), 889-910.

Ho, J.C.M. and Pam, H.J. (2003), "Inelastic design of low-axially loaded high-strength reinforced concrete columns", *Eng. Struct.*, **25**(8), 1083-1096.

Huang, C.S., Yeh, Y.K., Liu, G.Y., Hu, H.T., Tsai, K.C., Weng, Y.T., Wang, S.H. and Wu, M.H. (2002), "Axial load behavior of stiffened concrete-filled steel columns", *J. Struct. Eng.*, **128**(9), 1222-1230.

Johansson, M. (2002), "The efficiency of passive confinement in cft columns", *Steel Compos. Struct.*, **2**(5), 379-396.

Kwan, A.K.H. (2000), "Use of condensed silica fume for making high-strength, self-consolidating concrete", *Can. J. Civil Eng.*, **27**(4), 620-627.

Lai, M.H. and Ho, J.C.M. (2013), "Improving steel-concrete interface bonding in single-skinned high-strength concrete-filled-steel-tube columns by external steel rings", International Congress on Natural Sciences and Engineering (ICNSE 2013), Paper NSE309, 8-10 Jan, Taipei, Taiwan.

Lai, M.H. and Ho, J.C.M. (2014a), "Behaviour of uni-axially loaded concrete-filled-steel-tube columns confined by external rings", The Structural Design of Tall and Special Buildings, **23**(6), 403-426.

Lai, M.H. and Ho, J.C.M. (2014b), "Confinement effect of ring-confined concrete-filled-steel-tube columns under uni-axial load", *Eng. Struct.*, **67**, 123-141.

Li, B., Park, R. and Tanaka, H. (1991), "Effect of confinement on the behaviour of high strength concrete columns under seismic loading", *Paper presented at the Pacific Conference on Earthquake Engineering*, Auckland, 67-78.

Liao, F.Y., Han, L.H. and He, S.H. (2011), "Behavior of cfst short column and beam with initial concrete imperfection: Experiments", *J. Construct.Steel Res.*, **67**(12), 1922-1935.

Mehrparvar, B. and Khoshnoudian, F. (2011), "Efficiency of active systems in controlling base-isolated buildings subjected to near-fault earthquakes", *Struct. Des. Tall Spec.l Build.*, **20**(8), 1019-1034.

O'Shea, M.D. and Bridge, R.Q. (2000), "Design of circular thin-walled concrete filled steel tubes", *J. Struct. Eng.*, **126**(11), 1295-1303.

Pam, H.J. and Ho, J.C.M. (2009), "Length of critical region for confinement steel in limited ductility high-strength reinforced concrete columns", *Eng. Struct.*, **31**(12), 2896-2908.

Pam, H.J., Kwan, A.K.H. and Islam, M.S. (2001), "Flexural strength and ductility of reinforced normal-and high-strength concrete beams", Proceedings of the Institution of Civil Engineers. Structures and buildings, 146(4), 381-389.

Richart, F.E., Brandtzæg, A. and Brown, R.L. (1929), "The failure of plain and spirally reinforced concrete in compression", Illinois, USA: University of Illinois at Urbana Champaign.

Sakino, K., Nakahara, H., Morino, S. and Nishiyama, I. (2004), "Behavior of centrally loaded concrete-filled steel-tube short columns", *J. Struct. Eng.*, ASCE, **130**(2), 180-188.

Schneider, S.P. (1998), "Axially loaded concrete-filled steel tubes", *J. Struct. Eng.*, **124**(10), 1125-1138.

Tan, K.F. (2006), "Analysis of formulae for calculating loading bearing capacity of steel tubular high strength concrete", *J. Southwest Univ.Sci.Tech.*, **21**(2), 7-10 (in Chinese).

Xue, J.Q., Briseghella, B. and Chen, B.C. (2012), "Effects of debonding on circular cfst stub columns", *J. Construct. Steel Res.*, **69**(1), 64-76.

Zhong, S.T. (2006), "Unified theory of CFST: Research and application", Tsinghua University Press, Beijing, China (in Chinese).

Zhou, K.J.H., Ho, J.C.M. and Su, R.K.L. (2010), "Normalished rotation capacity for deformability evaluation of high-performance concrete beams", *Earthq. Struct.*, **1**(3), 269-287.

IT

List of notations

α	Strength ratio
β	Stiffness ratio
ξ_t	Confinement index
φ	Internal friction angel
ε_{sr}	Strain of steel rings
$\sigma_{s\theta}$	Hoop stress provided by the steel tube
σ_{sy}	Yield stress of the steel tube
σ_{sz}	Axial stress of the steel tube at yield condition (biaxial condition)
A_c	Contact concrete area
A_s	Contact steel area
A_{st}	Equivalent total steel area (taken into account the effect of external steel rings)
CFST	Concrete-filled-steel tube
d	Diameter of the steel rings, 8 mm
D_o	Outer diameter of the steel tube
E_{sr}	Elastic modulus for steel rings
f_c'	Unconfined concrete cylinder strength
f_{cc}	Confined concrete stress
f_r	Confining pressure
f_{yr}	Yield stress of rings
H	Height of the steel tube
HSC	High-strength concrete
HSCFST	High-strength concrete-filled-steel-tube
k	Confining coefficient related to the internal friction angel, φ
LS	Lateral strain
LVDT	Linear variable differential transducer
N_{exp}	Ultimate strength of HSCFST columns
N_{pre}	Predicted ultimate strength of HSCFST columns
NSC	Normal-strength concrete
RC	Reinforced concrete
S	Spacing of the rings
t	Thickness of the steel tube
UHSC	Ultra-high-strength concrete